Am J Transl Res 2020;12(10):6187-6203
www.ajtr.org /ISSN:1943-8141/AJTR0113057

Original Article

ΔNp63α promotes the expression and nuclear translocation of PTEN, leading to cisplatin resistance in oral cancer cells

Ting Hao[1,2], Ye-Hua Gan[1,2]

[1]*Central Laboratory,* [2]*Department of Oral & Maxillofacial, Peking University School and Hospital of Stomatology, 22 Zhongguancun Avenue South, Haidian District, Beijing 100081, China*

Received April 22, 2020; Accepted September 3, 2020; Epub October 15, 2020; Published October 30, 2020

Abstract: Pan-histone deacetylase (HDAC) inhibitors can induce the expression of phosphatase and tensin homolog deleted on chromosome 10 (PTEN) protein. However, the underlying mechanism by which this occurs remains unclear. In this study, we show that pan-HDAC inhibitors, including trichostatin A, suberoylanilide hydroxamic acid, and sodium butyrate, were able to induce PTEN mRNA and protein expression via the acetylation of the transcription factor ΔNp63α by inhibiting HDAC1 and HDAC3. ΔNp63α enhanced PTEN promoter activity by binding two newly identified recognition sites on it. Unfortunately, the inhibition of HDAC1 or HDAC3 failed to activate PTEN, as knockdown of HDAC1 inhibited both membrane-bound and nuclear PTEN, and knockdown of HDAC3 only induced cytoplasmic PTEN. Furthermore, the overexpression of ΔNp63α downregulated membrane-bound PTEN but enhanced the nuclear translocation of PTEN, leading to the cisplatin resistance of oral cancer cells. PTEN accumulated in the nuclei of cancerous cells and normal cells when ΔNp63α was highly expressed in specimens from patients with squamous cell carcinoma of the tongue. However, inhibiting either HDAC1 or HDAC6 prevented the nuclear translocation of PTEN and attenuated cisplatin resistance. These results suggest that chemotherapeutic inhibitors of HDAC1 or HDAC6, together with cisplatin, might improve outcomes for patients with squamous cell carcinoma of the tongue.

Keywords: ΔNp63α, PTEN, cisplatin resistance

Introduction

Phosphatase and tensin homolog deleted on chromosome 10 (PTEN) is recognized as a tumor suppressor due to its negative regulation of the phosphatidylinositol-4, 5-bisphosphate 3-kinase (PI3K)/protein kinase B (AKT) signaling pathway [1]. The major target of PTEN is phosphatidylinositol (3, 4, 5)-triphosphate (PIP3), which is generated by PI3K and acts as a bridge to recruit 3-phosphoinositide-dependent protein kinase 1 (PDK1) and AKT to the plasma membrane, further activating AKT by phosphorylation at its T308 site [2-4]. PTEN converts PIP3 into PIP2, interrupting the interaction between PDK1 and AKT, and thus negatively mediating the activation of AKT. Apart from its membrane-bound form, nuclear PTEN has multiple functions, including the induction of cell cycle arrest by inhibiting cyclin D1 expression [5], maintenance of chromosomal stability, and DNA double-strand break repair [6].

Low expression levels of PTEN are often associated with poor prognosis in patients with oral cancer [7, 8]; thus, enhancing its expression might improve the outcomes for such patients. Several transcription factors, including p53, egr-1, and PPARγ, bind the PTEN promoter and induce its transcription [9-11]. Further, our previous study showed that trichostatin A (TSA), a pan-histone deacetylase (HDAC) inhibitor, induced PTEN expression in oral cancer cells [12], but the transcription factor responsible for this induction remains unknown. Leonard et al. [13] reported that the transcription factor ΔNp63α inhibits PTEN expression in keratinocytes; these authors confirmed that ΔNp63α could bind the PTEN promoter between nucleotides -1703 and -1336 (transcription start site: +1). In this study, we wanted to deter-

mine whether p63 could contribute to the mediation of PTEN expression by pan-HDAC inhibitors.

P63 is a member of the p53 family. It contains two promoters and encodes two different proteins: the full-length trans-activating (TA) p63 and the N-terminally truncated (ΔN) p63 [14]. As different splice variants at the 3' end, both TAp63 and ΔNp63 have three protein variants (α, β, γ) each [15]. The distribution of p63 varies by tissue and cell types [16]. Specifically, ΔNp63 is highly expressed in epithelial cells, whereas TAp63 is expressed in B lymphoma cells. Just as in normal tissues, ΔNp63 is highly expressed in squamous cell carcinoma, and TAp63 is expressed in lymphoma [16, 17]. Furthermore, the α isoforms are the predominantly expressed variants, whereas the expression levels of the β and γ isoforms are expressed at very low levels [17]. The gene expression patterns regulated by p63 are also complicated. For example, TAp63α induces p21 expression, whereas ΔNp63α inhibits p21 expression [18]. However, ΔNp63α upregulates the expression of MKP3, Hsp70, and caspase-1 [19-21]. Furthermore, post-translational modifications of p63 usually affect its function and stabilization. Acetylation of p63 occurs when cells are at a high density, which slows the rate of cell proliferation by inducing p21 expression [22]. HDAC1 and HDAC2 have been shown to interact with p63 and mediate its gene expression levels [23], and p63 was found to be induced by HDAC inhibitors [24]. Therefore, we speculated that p63 might mediate the induction of PTEN by pan-HDAC inhibitors.

Considering that classic HDACs have 11 members, we investigated these HDACs by performing either pan-HDAC or selective inhibitors, to identify the specific isoforms of p63 involved in the mediation of PTEN expression. Besides PTEN expression, we also explored the role of PTEN translocation (mediated by HDACs and/or p63) after treatment of oral cancer cells with pan-HDAC inhibitors.

Materials and methods

Cell lines

WSU-HN6 and CAL27 cells derived from squamous cell carcinoma cells of the tongue, HeLa cells from human cervical cancer cells, and 293T cells from human embryonic kidney cells were cultured in Dulbecco's Modified Eagle's Medium (GIBCO, Grand Island, NY, USA) containing 10% fetal bovine serum at 37°C with 5% CO_2. All cell lines mentioned above were obtained from the American Type Culture Collection (Manassas, USA).

Reagents and antibodies

TSA and sodium butyrate were purchased from Sigma-Aldrich (St. Louis, MO, USA). SAHA, FK-228, tubastatin, cisplatin, CAY10683, RGF966, PCI34051, and MC1568 were purchased from Selleck Chemicals (Houston, TX, USA). Leptomycin B was purchased from Cell signaling Technology (Danvers, MA, USA). Anti-PTEN antibodies (#9552), anti-p63α rabbit monoclonal antibodies (#13109), anti-ΔNp63 rabbit monoclonal antibodies (#67825), anti-phospho-AKT (T308) rabbit monoclonal antibodies (#13038), anti-phospho-AKT (S 473) rabbit monoclonal antibodies (#4060), and anti-AKT (pan) rabbit monoclonal antibodies (#4685) were purchased from Cell Signaling Technology (Danvers, MA, USA). Anti-β-actin (I-19) antibodies (sc-1616), anti-HDAC1 antibodies, and anti-HDAC3 antibodies were purchased from Santa Cruz Biotechnology (Santa Cruz, CA, USA). Anti-p63 rabbit polyclonal antibodies (#12143-1-AP) and anti-cyclin D1 antibodies (#60186-1-Ig) were purchased from the Proteintech Group (Rosemont, IL, USA).

Plasmid constructs

The six isoforms of p63 cDNA were amplified using a high-fidelity DNA polymerase (TOYOBO, Osaka, Japan) and standard polymerase chain reaction (PCR) methods. The amplified fragments were digested with restriction enzymes and cloned into the pEGFP-C1 vector at the *Xho*I and *Bam*HI sites. ΔNp63α fragments were digested with restriction enzymes *Xho*I and *Bam*HI from the constructs described above and then cloned into the plvx-AcGFP-N1 vector. The sequence for p63 shRNA was 5'-GAT CAC CGT TTC GTC AGA ACA CAC ATC TCG AGA TGT GTG TTC TGA CGA AAC GGT TTT TT-3'. The sequence for HDAC1 shRNA was 5'-GAT CGC GTT CTT AAC TTT GAA CCA TAC TCG AGT ATG GTT CAA AGT TAA GAA CGT TTT T-3'. The sequence for HDAC3 shRNA was 5'-GAT CGA CCT AGT GTC CAG ATT CAT CTC GAG ATG AAT CTG GAC ACT AGG TTT TTT-3'. The double

strands oligonucleotides mentioned above were cloned into the plvx-shRNA1 vector. All plasmids were confirmed by sequencing.

Transient transfection

Cells were seeded into 6-well plates at a density of 1×10^6 per well. After the cells reached 95% confluence, they were transfected with 2 μg plasmids using Lipofectamine 3000 (Invitrogen), according to the manufacturer's instructions. The cells were harvested 48 h after transfection.

Lentivirus infection

Stable expression plasmids were co-transfected with lentiviral packing plasmids (Clontech) into 293T cells. Lentiviral supernatants were collected 48 h after transfection and then filtered with a 0.22-μm filter. The supernatant was added to target cells. The cells were screened with 1 μg/mL puromycin 48 h after infection and then incubated using medium containing 0.1 μg/mL puromycin.

Western blot analysis

Cells were washed three times with PBS and then collected in NP-40 lysis buffer (150 mM NaCl; 1% NP-40; and 50 mM Tris, pH 8.0). Protein concentrations were determined using the BCA (Thermo Fisher) method according to the manufacture's instruction. Equal amounts (15 μg) of protein were subjected to 10% sodium dodecyl sulfate-polyacrylamide gel electrophoresis and transferred onto a polyvinylidene fluoride membrane (Millipore, Billerica, MA, USA). The membrane was blocked with 5% nonfat milk in TBS-T (50 mM Tris, pH 7.5; 150 mM NaCl; and 0.05% Tween 20) for 1 h at room temperature. The membrane was incubated with primary antibodies (1:1000) in TBS-T at 4°C for 16 h, washed with TBS-T three times, and then incubated with horseradish peroxidase-conjugated secondary antibodies at room temperature for 1 h. After extensive washes with TBS-T, proteins on the membrane were visualized using enhanced chemiluminescence plus reagents (Thermo Fisher) and the FUSION FX imaging system (VILBER, France). The densitometry of each target band was assessed using Image J software, compared with an internal control, and then compared to the control groups to calculate the fold change in target protein expression.

Real-time quantitative PCR

Total RNA was extracted using the TRIzol reagent (Invitrogen). Reverse transcription was performed using a RevertAid RT Reverse Transcription Kit (Thermo Fisher), and real-time PCR was performed using the FastStart Universal SYBR Green Master mix (Roche), following the manufacturer's instructions. The primers for human PTEN are as follows: 5'-GAC CAT AAC CCA CAG C-3' (sense) and 5'-CCA GTT CGT CCC TTT CCA G-3' (antisense). The primers for human β-actin are as follows: 5'-CGG GAA ATC GTG CGT GAC-3' (sense) and 5'-CAG GCA GCT CGT AGC TCT T-3' (antisense). All primers were designed using Primer Premier software, version 5.0. Primer efficiency was confirmed by sequencing their conventional PCR products. Real-time PCR was performed using the 7500 real-time PCR system (Applied Biosystems).

Chromatin immunoprecipitation assay

The chromatin immunoprecipitation (ChIP) assay was performed using a ChIP assay kit (Millipore). Briefly, WSU-HN6 cells were cross-linked with 1% formaldehyde. The chromatin was sonicated into fragments, ranging between 200 and 1,000 bp, and then pulled down using anti-p63 antibodies for PCR amplification. The primers for amplifying the fragments (-1178 to -1031, translation start site designed as +1) containing both predicted p63-binding sites of the PTEN promoter are as follows: 5'-CTG CAG GCT GGC TGG GA-3' (sense) and 5'-AGG GCA GGG CAG GGC A-3' (antisense). Input was preserved from the sonicated fragments in a 5-μL volume. The PCR conditions used are as follows: A total of 35 cycles were performed, each consisting of 30 s at 94°C, 30 s at 55°C, and 30 s at 72°C. The PCR products were analyzed on a 1.5% agarose gel and then photographed.

DNA affinity purification assay

A DNA affinity purification assay was performed, as described previously [25]. Briefly, 5'-end-biotinylated oligonucleotides were custom synthesized, corresponding to the sequence of the PTEN promoter (-1160/-1140 region) A site (5'-biotin/GAA CCG GCC CGA GCA

AGC CC-3') and (-1052/-1032 region) B site (5'-biotin/CCC CCT GCC CTG CCC TGC CCT-3'). Then, 1.125 nmol of the biotinylated sense strand was annealed to its unlabeled antisense strand and incubated with 200 μg WSU-NH6 cell nuclear extracts. The DNA protein complex was precipitated using 100 μL streptavidin-conjugated agarose beads (S1638, Sigma-Aldrich). The bound proteins were released by boiling the beads in sodium dodecyl sulfate loading buffer and then subjected to western blot analysis.

Immunoprecipitation

The cells were washed three times with ice-cold, phosphate-buffered saline and placed in nondenaturing lysis buffer (20 mM Tris-HCl, pH 8.0, 137 mM NaCl, 1% nonidet P-40, and 2 mM EDTA). Equal amounts (500 μg) of whole-cell lysates were pre-incubated with 50 μL protein A/G agarose beads (Santa Cruz Biotechnology) for 1 h, and then the supernatants were incubated with 5 μg primary antibodies for 16 h with gentle rotation at 4°C. After the addition of 70 μL protein A/G agarose beads, the mixture was further incubated with gentle rotation for 4 h at 4°C and then centrifuged (12,000 × *g* for 1 min). The beads were washed five times with washing buffer (10 mM Tris, pH 7.4, 1 mM EDTA, 1 mM EGTA, pH 8.0, 150 mM NaCl, 1% Triton X-100, and 0.2 mM sodium orthovanadate). The protein-bead complex was eluted by boiling in the same volume of 2 × sodium dodecyl sulfate loading buffer and then subjected to western blot analysis.

Luciferase assay

The PTEN promoter reporter was constructed [26], and the luciferase assay was performed, as described previously [25]. Briefly, 1 μg PTEN reporter plasmid was transfected with Lipofectamine 3000 into WSU-HN6 cells in a 12-well plate. The transfected cells were lysed in cell lysis buffer (Promega) 24 h after transfection. Luciferase activity was measured using a FB12 luminometer (Berthold, Germany) with luciferin as the substrate, according to the manufacturer's instructions (Promega).

CRISPR/Cas 9 knockout of p63

The E-CRISP (http://www.e-crisp.org/E-CRISP/) program was used to design guided RNA (gRNA) pairs targeted to exon 3 of the p63 gene. The sequences for p63 sgRNA pairs were 5'-CAC CGT AGA GTT TCT TCA GTT CAG-3' and 5'-CAC CGA CAT GCC CCA TCC AGA TCA-3'. Oligonucleotides were synthesized and annealed to their antisense strands, and then cloned into the PX-458 and PX-459 vectors, respectively. Both plasmids were co-transfected into WSU-HN6 cells, and puromycin (1 μg/mL) was added 24 h after transfection to select positive cells. The culture medium was changed 48 h after the selection reagent was added. Genomic DNA was extracted, and the sgRNA targeting region was amplified by PCR. The products were sequenced and compared to the original sequence to verify that the target DNA had been cut by CRISPR/Cas 9.

Development of tumors from inoculated cells

Immunodeficient mice (BALB/c, male, 5 weeks old) were purchased from Beijing Vital River Laboratory Animal Technology Co. Ltd (Beijing, China). The care and treatment of experimental animals followed the institutional guidelines. Mice were randomly allocated to two groups (n = 10). WSU-HN6 control cells (vector only) and WSU-HN6 cells overexpressing ΔNp63α (2×10^6 cells/mouse) were subcutaneously inoculated into the right back flanks of each group of 10 mice, respectively. After 2 weeks, half of the mice in each group were separated and intraperitoneally injected with cisplatin (5 mg/kg, dissolved in saline), twice per week for 3 weeks. Saline was intraperitoneally injected at the same frequency in the other half of the mice. The mice were subsequently killed, and the weights of the tumors that developed were measured.

Immunofluorescence

Clinical specimens of squamous cell carcinoma and adjacent normal tissues were collected from 10 surgical patients in the Department of Oral and Maxillofacial Surgery, Peking University School of Stomatology. The paraffin-embedded specimens were sliced into 5-μm sections and mounted onto poly-L-lysine-coated slides. All specimens underwent a pathological diagnosis and contained carcinoma and precancerous tissues. The specimens were stained with hematoxylin-eosin (Figure S4), and the diagnosis was confirmed by experienced pathologists prior to immunofluorescence analyses. After

deparaffinization and antigen retrieval, the sections were blocked in 5% goat serum for 1 h and then incubated with primary antibodies (1:1000) at 4°C overnight. The sections were then incubated with tetramethylrhodamine-conjugated secondary antibodies (1:200) and fluorescein-conjugated secondary antibodies (1:200) the next day for 1 h and then washed with phosphate-buffered saline. Mounting medium containing DAPI was added to sections, and the samples were surveyed. The locations of p63, PTEN, and the nucleus were visualized using a Zeiss (Oberkochen, Germany) laser-scanning microscope (LSM 510) at wavelengths of 568 nm (60% power), 488 nm (60% power), and 405 nm (45% power). Images were processed using LSM 5 software, release 4.2. All images were obtained in the same profile setup to evaluate expression levels of each molecule. Images with high expression of p63 were observed to have bright red nuclei. Images with relatively low expression of p63 appeared a dull red, which was distributed throughout the whole cell. Relative fluorescence intensities of p63 and PTEN were measured using Image J software with the same threshold set, and nuclei were identified using DAPI with the same threshold set.

Cell viability assay

Cell viability assay was performed using Cell Counting Kit-8 (CCK-8, Dojindo, Kumamoto, Japan) according to the manufacturer's instructions. Briefly, the cells were seeded into 96-well plates (5×10^3 cells per well) and treated with or without the corresponding reagent. 48 h after treatment, 10 μl of CCK-8 reagent was added to each well and incubated at 37°C for 2 h. Absorbance at 450 nm was determined. Data was presented as relative absorbance at 450 nm compared to the control groups.

Coefficient of drug interaction

Determination of the coefficient of drug interaction (CDI) was performed, as described previously [27]. CDI was calculated as follows: CDI = AB/(A × B). AB is the ratio of the efficiency of the combination treatment groups compared to the control groups; A and B each represent the efficiency of the single drug treatment groups compared to the control groups. Thus, a CDI value less than 1, equal to 1, or greater than 1 indicates that the drugs are synergistic, additive, or antagonistic, respectively. A CDI value less than 0.7 indicates that the drugs have significantly synergistic effects.

Statistical analyses

Statistical analyses were performed using SPSS 22 for Windows. All experiments were repeated three times, and all data are presented as the mean ± standard deviation. Differences between multiple groups were analyzed by one-way analysis of variance. Homogeneity of variance test was performed before ANOVA analysis. When equal variance was assumed ($P > 0.05$), LSD (Least Significance Difference) method was performed as the post hoc test when ANOVA reach the significant level. A P value less than 0.05 was considered statistically significant.

Results

Pan-HDAC inhibitors induce the expression of PTEN and p63 in a dose- and time-dependent manner

As shown in **Figure 1**, PTEN mRNA expression was induced by the pan-HDAC inhibitor TSA in a dose- and time-dependent manner in WSU-HN6 cells. Protein expression of both PTEN and p63 were also induced by the pan-HDAC inhibitors TSA, suberoylanilide hydroxamic acid (SAHA), and sodium butyrate in a time- and dose-dependent manner. Unfortunately, we could not detect p63 protein expression using anti-p63α or anti-ΔNp63 antibodies in our western blot assays. Induction of PTEN protein expression by pan-HDAC inhibitors was also observed in CAL27 cells (Figure S1).

Pan-HDAC inhibitors induced PTEN protein expression via the acetylation of ΔNp63α at K297

To explore whether p63 was responsible for the induction of PTEN expression by pan-HDAC inhibitors, we either knocked down (or knocked out) p63 (the targeting sequence shared by all six isoforms) or overexpressed the six isoforms of p63 individually. The efficiency of shRNA or CRISPR/Cas 9 was confirmed by either western blot analysis or sequencing (Figure S2A-C). Knockdown of p63 by lentivirus-mediated shRNA not only inhibited PTEN mRNA and protein expression, but also blocked the effects of

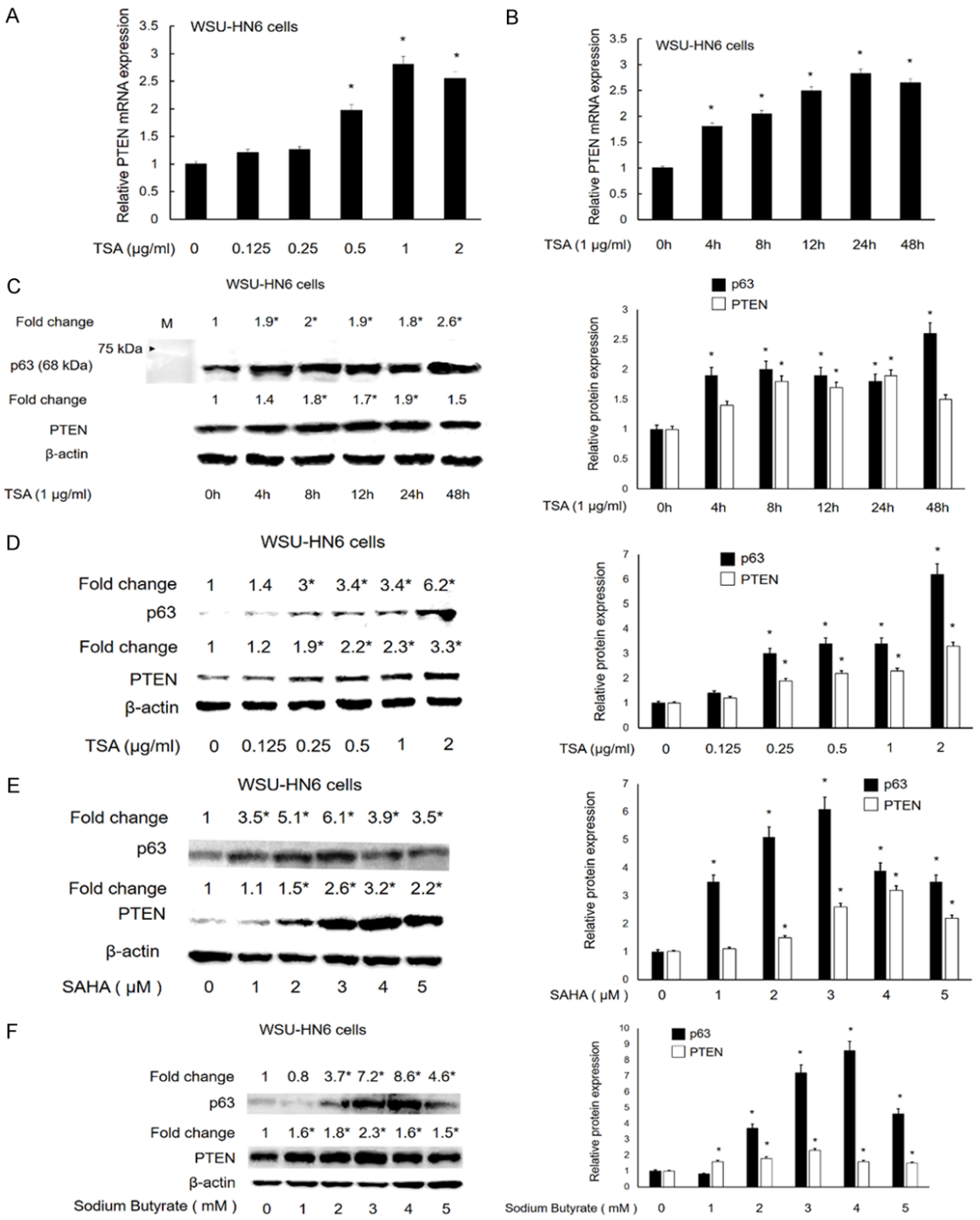

Figure 1. HDAC inhibitors induce PTEN expression in a time- and dose-dependent manner. (A) WSU-HN6 cells were treated with different doses of TSA for 24 h. PTEN mRNA expression levels were then assessed by real-time PCR. (B) Trichostatin A (TSA, 1 μg/mL) was added to WSU-HN6 cells and total RNA was extracted at predetermined time points. PTEN mRNA expression levels were then assessed by real-time PCR. The data are presented as the mean ± SD. **P* < 0.05 versus the control groups. (C) Cells were treated with TSA (1 μg/mL) for predetermined time points, (D) different doses of TSA for 24 h, (E) different doses of suberoylanilide hydroxamic acid (SAHA) for 24 h, and (F) different doses of sodium butyrate for 24 h. Protein expression levels of PTEN and p63 were then detected by western blot assay. β-actin served as an internal control for equal loading. Densitometry was performed to quantify the scanned bands. Data are shown as fold changes compared with the control group above the scanned bands. **P* < 0.05 versus the control group of the same series. M, marker.

TSA in WSU-HN6 and CAL27 cells (**Figure 2A**, **2B**, **2E-G**). Knockout of p63 by CRISPR/Cas 9 in HeLa cells further confirmed these results (**Figure 2C**). Transient overexpression of the six isoforms of p63 showed that only overexpressed ΔNp63α induced PTEN protein expression in WSU-HN6 cells (**Figure 2D**). Lentivirus-mediated stable overexpression of ΔNp63α further confirmed its induction of PTEN mRNA and protein expression. In addition, TSA enhanced the induction of overexpressed ΔNp63α in WSU-HN6 cells (**Figure 2E** and **2F**). Similar results were also observed in CAL27 cells (**Figure 2G**). To explore whether ΔNp63α-mediated PTEN expression transduced signals to downstream molecules, we assessed the expression of phospho-AKT (T308), a classical effector of PTEN. As shown in **Figure 2F**, p63 knockdown expectedly induced the phosphorylation of AKT on T308 after PTEN downregulation, whereas overexpression of ΔNp63α surprisingly upregulated the phosphorylation of AKT on T308, even though PTEN was induced by ΔNp63α. In the presence of TSA, however, only p63 knockdown reversed the inhibition of AKT phosphorylation on T308. In addition, phosphorylation of AKT on S473, which is not directly regulated by PTEN, was inhibited by p63 knockdown but was not induced by the overexpression of ΔNp63α, whereas inhibited by TSA.

The results above indicated that ΔNp63α was responsible for the induction of PTEN expression by pan-HDAC inhibitors. We next explored whether acetylation of ΔNp63α was involved in this process since HDACs could modify protein acetylation. Since ΔNp63α has been shown to be acetylated at both K281 and K297 [22], we constructed expression plasmids of ΔNp63α with the K281 and K297 sites mutated to either glutamine (to mimic its acetylation) or arginine (to abolish its acetylation) and overexpressed them in WSU-HN6 cells. As shown in **Figure 2H**, overexpression of ΔNp63α K281Q, K281R, or K297R all failed to affect PTEN protein expression, whereas overexpression of ΔNp63α K297Q induced PTEN protein expression to wild-type levels. In addition, overexpression of wild-type ΔNp63α, but not mutant ΔNp63α K297R, induced self-acetylation (Figure S2D). These results imply that the acetylation of ΔNp63α at K297 might be responsible for the induction of PTEN expression by pan-HDAC inhibitors. To confirm this hypothesis, we further overexpressed wild-type ΔNp63α, ΔNp63α K297Q, or ΔNp63α K297R in WSU-HN6 cells and in p63-knockout HeLa cells. As shown in **Figure 2I** and **2J**, TSA further induced PTEN protein expression in the presence of wild-type ΔNp63α or ΔNp63α K297Q, but not in the presence of ΔNp63α K297R, in both WSU-HN6 and p63-knockout HeLa cells. These results indicate that the acetylation of ΔNp63α at K297 is responsible for the ΔNp63α-mediated induction of PTEN protein expression by TSA.

ΔNp63α binds the PTEN promoter to induce PTEN promoter activity

We predicted two new binding sites (-1160/-1140 and -1052/-1032) for p63 on the PTEN promoter (since PTEN has nine transcription start points [28], its translation start site was designated +1). ChIP assays were performed using specific primers to amplify the predicted 146-bp region (-1178 to -1031) of the PTEN promoter. As shown in **Figure 3A**, the expected size of the DNA fragment was amplified from the chromatin pulled down by anti-p63 antibodies, but not by anti-IgG antibodies. We also performed a DNA affinity pull-down assay using two probes containing the two predicted binding sites: A (-1160/-1140) and B (-1052/-1032). **Figure 3B** shows that ΔNp63α was detected in the precipitates of both probes. PTEN promoter activity decreased when p63-binding site A, site B, or both sites were mutated compared to the wild-type site (**Figure 3C**). Overexpression of ΔNp63α only induced wild-type PTEN promoter activity by about 2-fold but failed to induce promoter activity from promoters containing p63-binding site mutations.

Inhibition of HDAC1 or HDAC3 induces PTEN protein expression but fails to activate PTEN

To identify the exact HDAC that contributed to the ability of acetylated ΔNp63α to regulate PTEN expression, we used several specific HDAC inhibitors to narrow down the candidates. As shown in **Figure 4A** and **4B**, FK228, an inhibitor of HDAC1 and HDAC2, and RGF 966, an inhibitor of HDAC3, both induced PTEN protein expression, whereas CAY10683, an inhibitor of HDAC2, PCI34051, an inhibitor of HDAC8, and MC1568, an inhibitor of class II HDACs (HDAC4, 5, 6, 7, 9, and 10), all failed to induce PTEN pro-

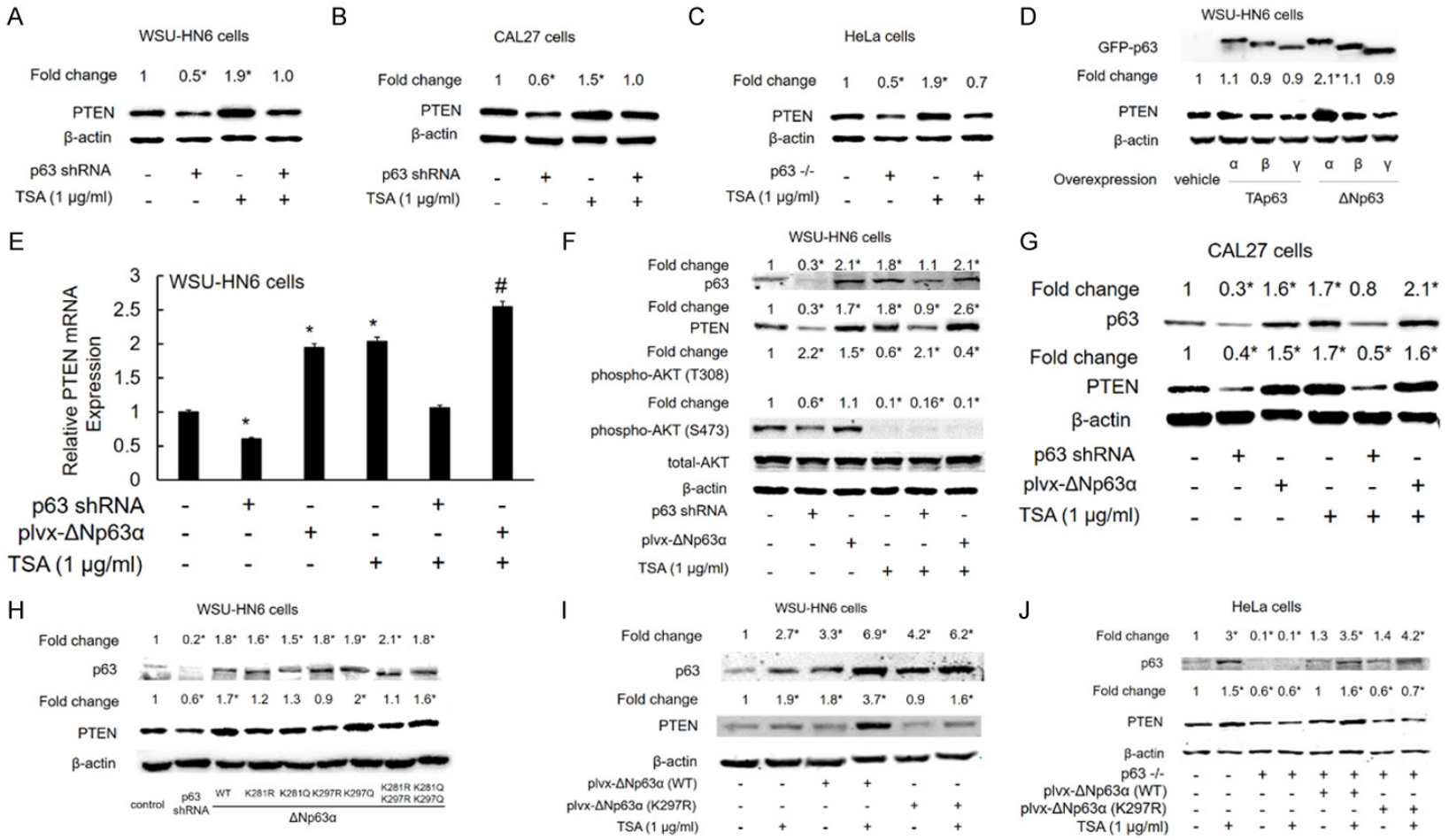

Figure 2. TSA induces PTEN expression by ΔNp63α acetylation at K297. P63 was stably knocked down by lentivirus-mediated shRNA (p63 shRNA) in either (A) WSU-HN6 cells or (B) CAL27 cells, or knocked out (p63 -/-) by CRISPR/Cas 9 in HeLa cells (C) before being treated with 1 μg/mL TSA for 24 h. Protein expression levels of PTEN were then detected by western blot assay. β-actin served as an internal control for equal loading. (D) Six isoforms of p63 were transiently overexpressed in WSU-HN6 cells for 24 h. P63 was stably knocked down (p63 shRNA), or ΔNp63α was stably overexpressed by lentivirus-mediated overexpressed plasmid (plvx-ΔNp63α), in WSU-HN6 cells (E and F) or in CAL27 cells (G) prior to being treated with 1 μg/mL TSA for 24 h. PTEN mRNA expression levels in WSU-HN6 cells were detected by real-time PCR (E). The data are presented as the mean ± SD. $*P < 0.05$ versus the control groups. (F and G) Total proteins were extracted and subjected to western blot analysis. β-actin served as an internal control for equal loading. Densitometry was performed to quantify the scanned bands. Data are shown as fold changes compared with the control group above the scanned bands. $*P < 0.05$ versus the control group. (H) Different acetylation site mutants of ΔNp63α were stably overexpressed in WSU-HN6 cells. Wild-type (WT) or non-acetylated (K297R) ΔNp63α was stably overexpressed in WSU-HN6 cells (I) or in p63-knockout Hela cells (J) and treated with 1 μg/mL TSA for 24 h. (+) stands for treatment described on the left was performed while (-) represents none of the treatment. Total proteins were extracted and subjected to western blot analyses. β-actin served as an internal control for equal loading. Densitometry was performed to quantify the scanned bands. Data are shown as fold changes compared with the control group above the scanned bands. $*P < 0.05$ versus the control group.

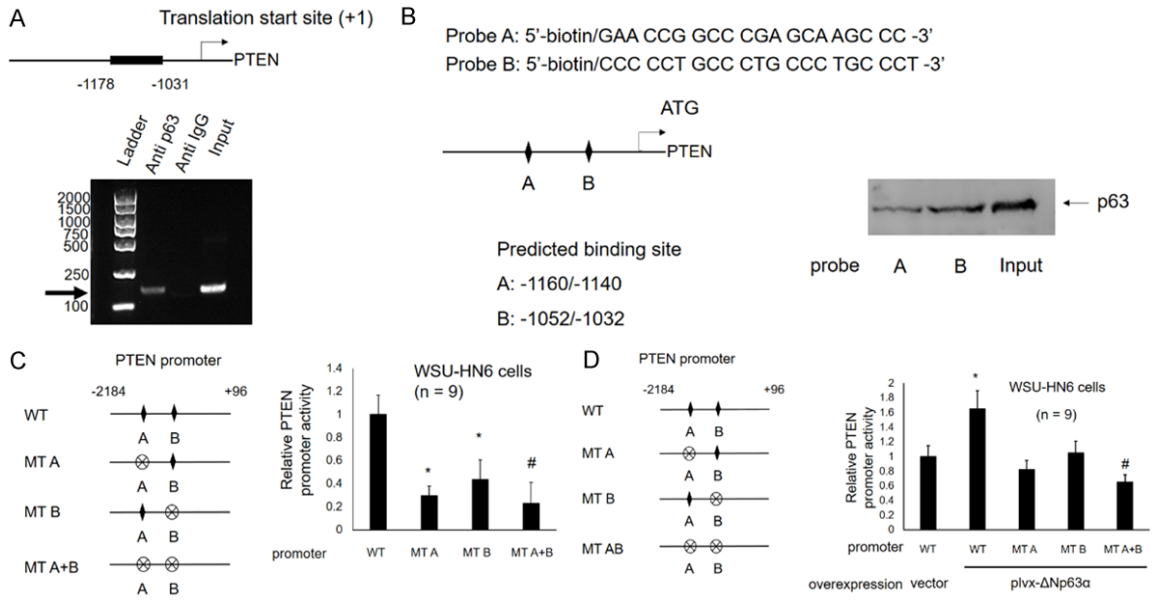

Figure 3. P63 binds the PTEN promoter and enhances its activity. A. Schematic of the -1178/-1031 region of the PTEN promoter containing both p63-binding sites. Results of ChIP performed using an anti-p63 antibody and primers amplifying the -1178/-1031 region. The black arrow points to the target band. B. Sequences of two probes corresponding to the predicted p63-binding sites of the PTEN promoter shown relative to the initiating ATG. The bound complex was pulled down by streptavidin-conjugated agarose and subjected to western blot analysis. P63 was detected by anti-p63 antibodies. C and D. Mutated p63-binding sites are represented by crossed circles. Cells were transfected with wild-type (WT) and mutant reporter constructs for 24 h. D. vector or ΔNp63α was overexpressed before reporter being transfected. Relative fluorescence intensity was calculated and data (mean ± SD of nine separate experiments) are shown as fold change compared to control group. *$P < 0.05$ versus the control group.

tein expression in WSU-HN6 and CAL27 cells, implying that only HDAC1 and HDAC3 were involved in regulating PTEN expression. These results were further confirmed by knockdown of HDAC1 or HDAC3 by lentivirus-mediated shRNA, which correspondingly induced PTEN protein expression (**Figure 4C**). We also showed that knockdown of HDAC1 or HDAC3 induced the acetylation of ΔNp63α (**Figure 4D**) and that ΔNp63α interacted with both HDAC1 and HDAC3, as shown in immunoprecipitation experiments (**Figure 4E**).

Although the inhibition of HDAC1 or HDAC3 induced PTEN expression, whether PTEN was activated by the inhibition of these two HDACs was unclear. As shown in **Figure 4F**, knockdown of HDAC1 inhibited membrane-bound PTEN (active form) and correspondingly induced membrane-bound AKT (active form) and phosphorylation of AKT on T308. Knockdown of HDAC3 showed little effect on membrane-bound PTEN or AKT. Knockdown of HDAC1 also inhibited nuclear PTEN but upregulated cytoplasmic PTEN, whereas knockdown of HDAC3 merely upregulated cytoplasmic PTEN. PTEN was not activated by the inhibition of HDAC1 or HDAC3, even though its expression was induced.

Overexpression of ΔNp63α induces PTEN nuclear translocation

Given the downregulation of membrane-bound PTEN after HDAC1 knockdown and the induction of the phosphorylation of AKT on T308 by ΔNp63α overexpression, we wanted to know how p63 affected the subcellular location of PTEN. As shown in **Figure 5A**, knockdown of p63 inhibited both membrane-bound and nuclear PTEN, whereas the overexpression of ΔNp63α more significantly inhibited membrane-bound PTEN but surprisingly induced nuclear PTEN. Correspondingly, the phosphorylation of AKT on T308, which is a target of membrane-bound PTEN, was induced 3.3-times by p63 knockdown but only 1.5-times by ΔNp63α overexpression (**Figure 5A**), suggesting that ΔNp63α overexpression less effectively affects AKT activity than p63 knockdown.

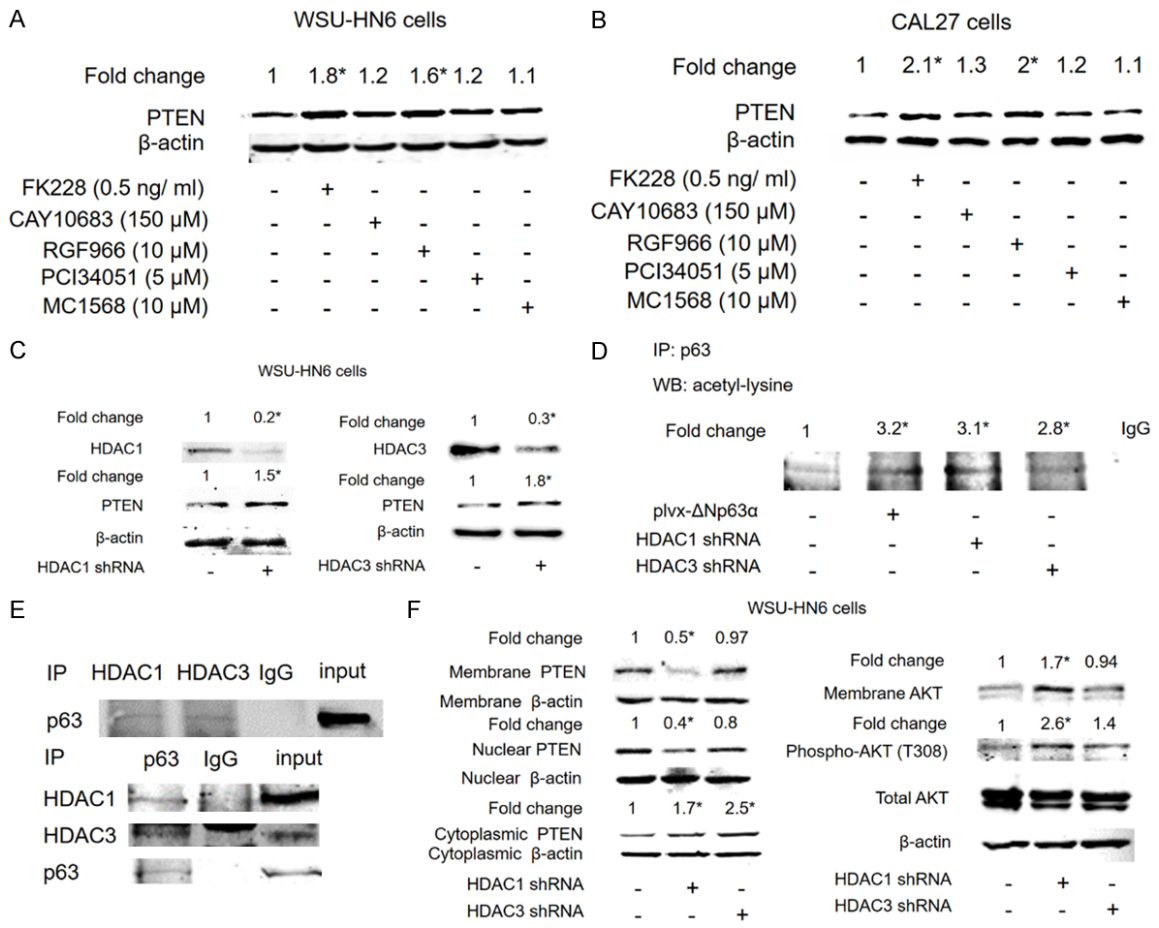

Figure 4. Inhibition of HDAC1 and HDAC3 induces but inactivates PTEN expression. (A) WSU-HN6 or (B) CAL 27 cells were treated with several specific HDAC inhibitors (FK228, an HDAC1 and HDAC2 inhibitor; CAY10683, an HDAC2 inhibitor; RGF966, an HDAC3 inhibitor; PCI34051, an HDAC8 inhibitor; and MC1568, a class II HDAC inhibitor) for 24 h. Total proteins were extracted and subjected to western blot analyses. β-actin served as an internal control for equal loading. Densitometry was performed to quantify the scanned bands. (C) HDAC1 or HDAC3 were stably knockdown by lentivirus-mediated shRNA in WSU-HN6 cells. Total proteins were extracted and subjected to western blot analyses. The protein expression levels of HDAC1, HDAC3 and PTEN were detected (D) ΔNp63α was stably overexpressed, and HDAC1 or HDAC3 was stably knocked down by lentivirus-mediated shRNA in WSU-HN6 cells, respectively. Total proteins were extracted and subjected to immunoprecipitation with an anti-p63 antibody and detected with an anti-acetyl-lysine antibody. Densitometry was performed to quantify the scanned bands. (E) HDAC1 and HDAC3 interacted with p63. IP, immunoprecipitation. WB, western blot. (F) HDAC1 or HDAC3 were stably knockdown by lentivirus-mediated shRNA. Total proteins (E) or separated cell components (F) were extracted and subjected to western blot analyses. Data are shown as fold changes compared with the control group above the scanned bands. *$P < 0.05$ versus the control group.

Meanwhile, p63 knockdown induced cyclin D1 protein expression, which is negatively regulated by nuclear PTEN and positively regulated by phosphorylated AKT [29]. The overexpression of ΔNp63α significantly inhibited cyclin D1 protein expression, consistent with results showing that ΔNp63α overexpression more significantly upregulated nuclear PTEN (by 2.8-times) than AKT phosphorylation (by 1.5-times). Similar results were also observed in CAL27 cells (**Figure 5B**). We also examined the proliferation rate of cancer cells overexpressing ΔNp63α to further confirm the induction of nuclear PTEN by ΔNp63α overexpression. As shown in **Figure 5C** and **5D**, ΔNp63α overexpression gradually inhibited cell proliferation in both WSU-HN6 and CAL27 cells, as expected.

To further examine whether ΔNp63α overexpression really induced PTEN nuclear translocation, we surveyed the locations of p63 and PTEN in specimens from 10 patients with squa-

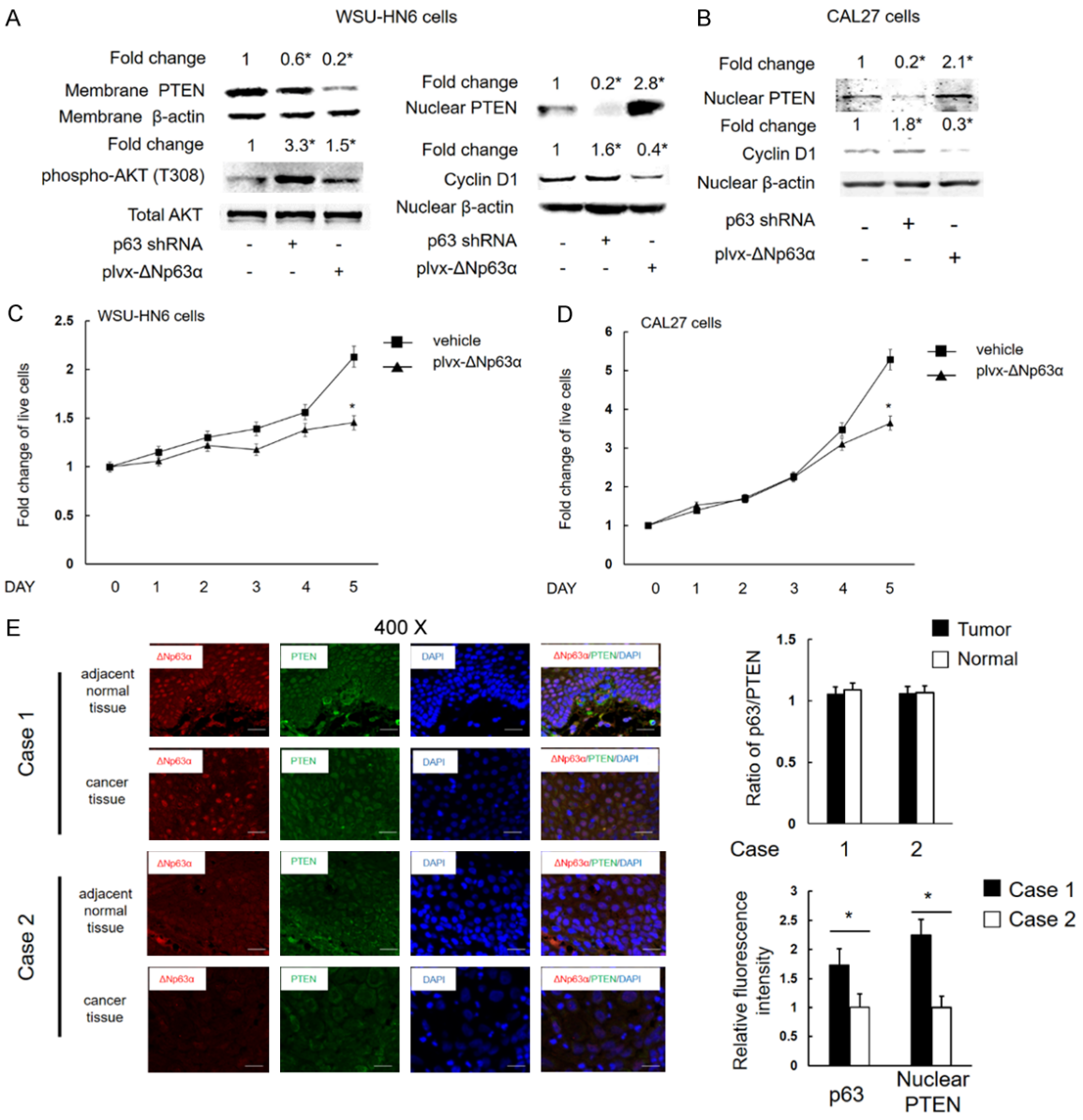

Figure 5. Overexpression of ΔNp63α induces PTEN nuclear translocation and inhibits cell proliferation rate. (A) P63 was stably knocked down or ΔNp63α was stably overexpressed in WSU-HN6 cells or (B) in CAL27 cells. Nuclear or membrane proteins were extracted and subjected to western blot analyses. Membrane-bond PTEN and nuclear PTEN were detected, and the corresponding downstream effectors were detected. (C) WSU-HN6 or (D) CAL27 cells with or without stably overexpressed ΔNp63α were seeded into a 96-well plate at a density of 500 cells/well. The optical absorbance at 450 nm in each well was detected. Data (mean ± SD of five separate experiments) are shown as the relative optical absorbance compared with the control groups. (E) Confocal photographs of immunofluorescent staining represented expression and location of p63 (red) and PTEN (green) in pathological sections from patients with squamous cell carcinoma of the tongue. DAPI (blue) was stained to identify the nucleus. The normal and malignant areas were in the same section in one case. Magnification = 400 X. Scale bar = 20 μm. Two representative cases are shown. Relative fluorescence intensity was measured by Image J software under the same threshold set. *$P < 0.05$ versus the control group.

mous cell carcinoma of the tongue by laser confocal microscopy. As shown in **Figure 5E**, the relative fluorescence intensity of p63 in the cancerous and precancerous tissues of the same patient was similarly either high (5/10) or low (5/10). In addition, PTEN co-localized with p63 in the nucleus when expression of p63 was high (5/10). However, nuclear PTEN was barely detectable in the nucleus when expression of p63 was low (5/10).

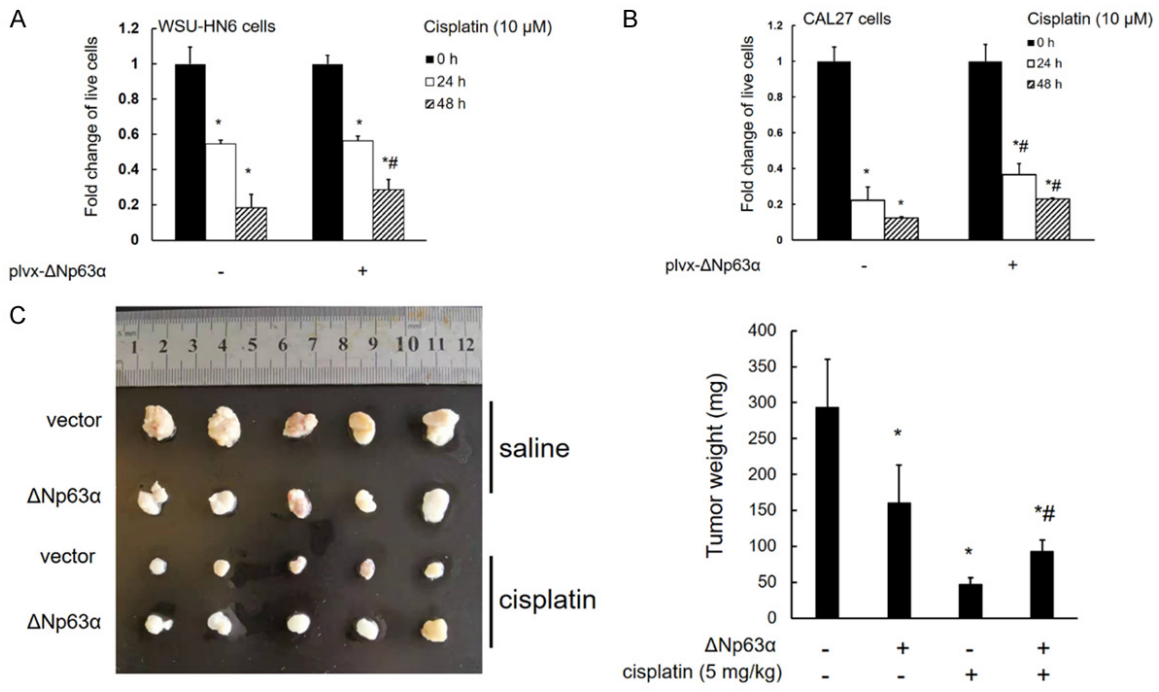

Figure 6. Overexpression of ΔNp63α contributes to cisplatin resistance (A) WSU-HN6 or (B) CAL27 cells with or without stably overexpressed ΔNp63α were seeded into a 96-well plate at a density of 5,000 cells/well and treated with 10 μM cisplatin for 24 or 48 h. A CCK-8 kit was used to count the number of cells in each well. Data (mean ± SD of five separate experiments) are shown as the relative number of live cells compared with the control group. *P < 0.05 versus the control group; #P < 0.05 versus the group with the same time set. (C) Photographs and weights of tumors that developed in the animals. Tumor growth that developed from cells stably transfected with ΔNp63α exhibited cisplatin resistance in nude mice. *P < 0.05 versus the control group; #P < 0.05 versus cisplatin treatment groups.

In addition, we further examined whether acetylation of ΔNp63α was involved in PTEN nuclear translocation. Unexpectedly, both acetylated (297Q) and nonacetylated (297R) forms of ΔNp63α induced nuclear PTEN (Figure S3), indicating that the acetylation of ΔNp63α at K297 was not involved in regulating PTEN nuclear translocation.

Overexpression of ΔNp63α contributes to cisplatin resistance

Since nuclear PTEN functions as a DNA damage repair molecule [30] and overexpression of ΔNp63α induces the nuclear translocation of PTEN, we speculated that ΔNp63α overexpression might enhance cisplatin resistance. As shown in **Figure 6A** and **6B**, the relative live cells with overexpression of ΔNp63α was significant higher at 48 h (about 48%) after treatment with cisplatin in WUS-HN6 cells or at 24 h (about 65%) after treatment with cisplatin in CAL27 cells than in control cells. Similarly, the average weight of the tumors that developed was 2-fold higher in animals with ΔNp63α-overexpressing cells treated with cisplatin compared to those treated with cisplatin alone (**Figure 6C**). In addition, the average weight of the tumors that developed in the ΔNp63α-overexpressing animals was lower than that of the control animals, further confirming that the overexpression of ΔNp63α slows the proliferation of squamous cell carcinoma cells of the tongue (**Figure 6C**).

Inhibition of HDAC1 or HDAC6 reverses cisplatin resistance by excluding PTEN from the nucleus

Since the overexpression of ΔNp63α induces PTEN nuclear translocation and is involved in cisplatin resistance, we next examined whether the inhibition of HDACs would exclude PTEN from the nucleus and sensitize cisplatin in squamous cell carcinoma cells of the tongue. GAPDH and lamin B1 were tested by western blot to avoid cytoplasmic contamination of nuclear extracts (Figure S6A) previously. As

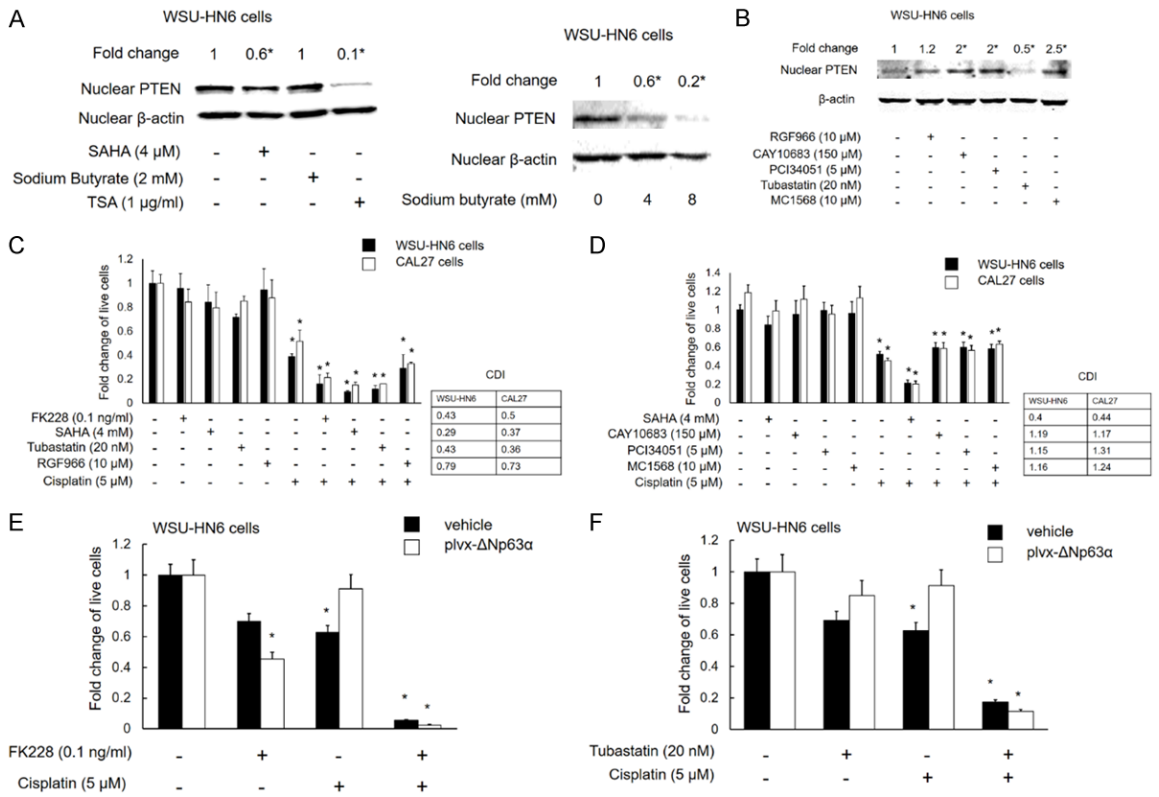

Figure 7. Inhibition of HDAC1 or HDAC6 reverses cisplatin resistance by excluding PTEN from the nucleus. A and B. WSU-HN6 cells were treated with several HDAC inhibitors (TSA, SAHA, and sodium butyrate, pan-HDAC inhibitors, CAY10683, an HDAC2 inhibitor; RGF966, an HDAC3 inhibitor; PCI34051, an HDAC8 inhibitor; tubastatin, an HDAC6 inhibitor, and MC1568, a class II HDAC inhibitor) at the indicated doses for 24 h. Nuclear proteins were extracted and subjected to western blot analyses. Nuclear PTEN was detected. C and D. WSU-HN6 cells or CAL27 cells were seeded into a 96-well plate at a density of 5,000 cells/well and treated with the HDAC inhibitors listed, cisplatin, or a combination of cisplatin and the HDAC inhibitors for 48 h. Relative live cells were calculated and represented as percentage of the control groups. E. WSU-HN6 cells overexpressing ΔNp63α (plvx-ΔNp63α) or vehicle were seeded into a 96-well plate at a density of 5,000 cells/well and treated with FK228, cisplatin, or a combination of FK228 and cisplatin for 48 h. Relative live cells were calculated and represented as percentage of the control groups. F. WSU-HN6 cells overexpressing ΔNp63α or vehicle were seeded into a 96-well plate at a density of 5,000 cells/well and treated with tubastatin, cisplatin, or a combination of tubastatin and cisplatin for 48 h. Relative live cells were calculated and represented as percentage of the control groups. A CCK-8 kit was used to count the number of cells in each well. Data (mean ± SD of five separate experiments) are shown as the relative number of live cells compared with the control group. CDI, coefficient of drug interaction. *$P < 0.05$ versus the control group of the same series.

shown in **Figure 7A** and **7B**, the pan-HDAC inhibitors TSA, SAHA, and sodium butyrate (at high doses), and the HDAC6-specific inhibitor tubastatin all inhibited the nuclear translocation of PTEN, whereas CAY10683, PCI34051, and MC1568 all induced its nuclear translocation. Meanwhile, RGF966 (a specific inhibitor or HDAC3) showed little effect on PTEN nuclear translocation. These results, together with the results shown in **Figure 4F**, suggest that only the inhibition of HDAC1 or HDAC6 inhibits the nuclear translocation of PTEN.

According to the results above, we investigated several combinations of different HDAC inhibitors with cisplatin to assess whether they would enhance the inhibitory effects of cisplatin on cancer cell proliferation. As shown in **Figure 7C** and **7D**, the combination of cisplatin and SAHA, tubastatin, or FK228 all synergistically inhibited cell proliferation, whereas the combination of cisplatin with RGF966 showed little synergistic inhibitory effects on proliferation. Furthermore, CAY10683, PCI34051, and MC1568 antagonized the inhibitory effects of cisplatin on cell proliferation. In addition, we further observed that cells pretreated with the nuclear protein export inhibitor leptomycin B, which also induced nuclear PTEN (Figure S5A), blocked the synergistic inhibitory effects of the

combination of cisplatin and SAHA, tubastatin, or FK228 on cell proliferation (Figure S5B and S5C). However, both FK228 and tubastatin abolished ΔNp63α overexpression-mediated cisplatin resistance (**Figure 7E** and **7F**). These results indicate that ΔNp63α overexpression contributes to cisplatin resistance by increasing nuclear PTEN; cisplatin resistance can be reversed by inhibiting HDAC1 or HDAC6.

Discussion

In the present study, we showed that pan-HDAC inhibitors induced PTEN expression via the acetylation of ΔNp63α at K297. The overexpression of ΔNp63α enhanced PTEN nuclear translocation, contributing to cisplatin resistance in squamous carcinoma cells of the tongue.

Pan-HDAC inhibitors induced PTEN expression by inhibiting HDAC1 and HDAC3. Understanding the mechanism underlying the pan-HDAC inhibitor-mediated induction of PTEN expression was our major objective. We observed that pan-HDAC inhibitors, including TSA, SAHA, and sodium butyrate, could induce both PTEN and p63 protein expression in WSU-HN6 and CAL27 cells, which are cell lines derived from squamous cell carcinoma cells of the tongue. Knockdown of p63 by lentivirus-mediated shRNA in these two cell lines and knockout of p63 by CRISPR/Cas 9 in HeLa cells inhibited PTEN protein expression and blocked TSA-induced PTEN protein expression, respectively. These results strongly suggest that p63 is involved in the TSA-stimulated induction of PTEN protein expression. Although the predicted molecular mass of ΔNp63α is 75 kDa and the p63 antibody does not distinguish between the six isoforms of p63, a band around 68 kDa, which was detected in the two cell lines, was consistent with the molecular mass of the p63 band, according to the antibody manufacturer, and could be ΔNp63α, considering that ΔNp63α is the only predominantly expressed isoform in epithelial or squamous cell carcinoma [17]. Moreover, when all six isoforms of p63 were overexpressed, only ΔNp63α was able to induce PTEN protein expression. Furthermore, the overexpression of ΔNp63α upregulated PTEN transcription by binding two recognition sites (-1160/-1140 and -1052/-1032) on the PTEN promoter and enhancing its activity. Point mutation experiments showed that the acetylation of ΔNp63α at K297 mediated the induction of PTEN expression by pan-HDAC inhibitors. The exact HDACs that induced PTEN expression were identified as HDAC1 and HDAC3 by selective inhibitors and knockdown experiments. In addition, HDAC1 and HDAC3 were responsible for the acetylation of ΔNp63α. Based on our results, ΔNp63α is a positive regulator of PTEN in squamous cell carcinoma cells of the tongue. However, these findings are in contrast to those of a previous study in which ΔNp63α inhibited PTEN expression in A431 cells (derived from an atypical squamous cell of human vulva epidermis) [13]. Future studies are needed to investigate whether ΔNp63α differentially regulates PTEN in different cell types.

The two binding sites of p63 on the PTEN promoter in this study differed from those identified in the study mentioned above. Leonard et al. identified two p63-binding regions on the PTEN promoter, which were located near the transcription start site, according to the NCBI reference sequences (NM_000314) of the PTEN Mrna [13]. However, the so-called transcription start site was -1030 bp away from the translation start site of PTEN. Therefore, their two binding sites were located at -2445/-2238 and -2853/-2638, respectively, when the translation start site was designed as +1. Our PTEN promoter gene sequence ranged from -2184 to +96 (translation start site designed as +1) and did not cover any region reported by Leonard et al. The role of these upstream binding sites must be confirmed in future studies.

ΔNp63α induced the nuclear translocation of PTEN, resulting in cisplatin resistance. Although the overexpression of ΔNp63α induced PTEN protein expression, it inhibited membrane-bound PTEN (active form) even more significantly than did the knockdown of p63 (**Figure 5A**). However, the knockdown of p63 induced the phosphorylation of AKT on T308 (active form) more significantly than did ΔNp63α overexpression (**Figure 5A**), implying that ΔNp63α signaling inhibited membrane-bound PTEN but not efficiently induced AKT phosphorylation on T308. These findings prompted us to examine whether the overexpression of ΔNp63α induced the nuclear translocation of PTEN. As expected, nuclear PTEN was upregulated and cyclin D1

expression was strongly inhibited, whereas p63 knockdown upregulated cyclin D1 (**Figure 5A**). Our results of the negative regulation of cyclin D1 by nuclear PTEN are consistent with results in a previous report [31], in which nuclear PTEN downregulated cyclin D1 via its phosphatase activity. Correspondingly, the overexpression of ΔNp63α slightly inhibited tumor cell proliferation both in vitro and in vivo (**Figures 5C**, **5D**, **6C**), possibly stimulating the nuclear translocation of PTEN induced by the overexpression of ΔNp63α. However, while the mechanism underlying the ΔNp63α-mediated induction of nuclear PTEN is unknown, it seems independent of the acetylation of ΔNp63α at K297 (Figure S3). Since nuclear PTEN maintains chromosomal stability and contributes to DNA double-strand break repair [6], the overexpression of ΔNp63α expectedly resulted in cisplatin resistance by approximately 48% in squamous cell carcinoma cells of the tongue. Our results are consistent with those of a previous study in which the overexpression of ΔNp63α caused cisplatin resistance by the upregulation of EGFR [32]. Therefore, these results suggest a new mechanism for conferring cisplatin resistance in oral cancer cells.

The inhibition of HDAC1 or HDAC6 reverses cisplatin resistance by excluding PTEN from the nucleus. Our results showed that only the inhibition of HDAC1 or HDAC6 could exclude PTEN and were synergistic with cisplatin in terms of its antitumor effects (**Figure 7C**); however, the inhibition of other HDACs did not show this synergistic effect with cisplatin treatment (**Figure 7D**). Furthermore, the HDAC inhibitors that induce nuclear PTEN are antagonistic with cisplatin. In addition, the synergistic effects of HDAC1 and HDAC6 were reversed by the addition of the nuclear protein export inhibitor, leptomycin B, which also induced nuclear PTEN (Figure S5). We also observed that the inhibition of HDAC1 or HDAC6 totally reversed cisplatin resistance, which had been induced by the overexpression of ΔNp63α (**Figure 7E** and **7F**). These results imply that cisplatin might more effectively treat oral cancers when combined with HDAC1 or HDAC6 inhibitors.

The mechanism by which PTEN is translocated to the nucleus is complicated. To date, several studies have reported that both phosphorylation and ubiquitination contribute to PTEN nuclear localization [29, 33]. Another study reported that the inhibition of HDAC1 enhances PTEN phosphorylation [34], which, depending on the site of phosphorylation, can inhibit its nuclear translocation [35]. However, the exact phosphorylation sites of PTEN regulated by the knockdown of HDAC1 are yet to be identified. Since we had reported that the inhibition of HDAC6 induced membrane-bound PTEN [36], the effects of the reduction of nuclear PTEN by the inhibition of HDAC6 might be offset by cytoplasmic PTEN, due to the lack of direct effects on PTEN expression by HDAC6. However, the exact mechanism by which HDACs regulate PTEN nuclear translocation are yet to be identified.

Lamin B1 is served as loading control of nuclear protein usually. However, in our study, HDAC inhibitors modified its expression significantly (Figure S6B). We need another loading control for our experiments. Several studies have reported that β-actin could be detected in nucleus [37-39], and we found that the expression of the molecule was not affected by the HDAC inhibitors. So β-actin was selected served as our loading control of nuclear protein.

In conclusion, ΔNp63α induces PTEN expression and nuclear localization, which contribute to cisplatin resistance in squamous cell carcinoma cells of the tongue. The inhibition of HDAC1 or HDAC6 could enhance the anticancer effects of cisplatin.

Acknowledgements

This work was supported by the National Natural Science Foundation of China (Grant Nos. 81472764 and 81271173) and the China International Science and Technology Cooperation (Grant No. 2013DFB30360).

Disclosure of conflict of interest

None.

Address correspondence to: Dr. Ye-Hua Gan, Central Laboratory, 22 Zhongguancun Nandajie, Haidian District, Beijing 100081, China. Tel: +86-10-8219-9977; Fax: +86-10-62173402; E-mail: kqyehuagan@bjmu.edu.cn

References

[1] Myers MP, Pass I, Batty IH, Van der Kaay J, Stolarov JP, Hemmings BA, Wigler MH, Downes CP and Tonks NK. The lipid phosphatase activity of PTEN is critical for its tumor supressor func-

tion. Proc Natl Acad Sci U S A 1998; 95: 13513-13518.
[2] Maehama T and Dixon JE. The tumor suppressor, PTEN/MMAC1, dephosphorylates the lipid second messenger, phosphatidylinositol 3,4, 5-trisphosphate. J Biol Chem 1998; 273: 13375-13378.
[3] Li J, Simpson L, Takahashi M, Miliaresis C, Myers MP, Tonks N and Parsons R. The PTEN/MMAC1 tumor suppressor induces cell death that is rescued by the AKT/protein kinase B oncogene. Cancer Res 1998; 58: 5667-5672.
[4] Stambolic V, Suzuki A, de la Pompa JL, Brothers GM, Mirtsos C, Sasaki T, Ruland J, Penninger JM, Siderovski DP and Mak TW. Negative regulation of PKB/Akt-dependent cell survival by the tumor suppressor PTEN. Cell 1998; 95: 29-39.
[5] Chung JH, Ostrowski MC, Romigh T, Minaguchi T, Waite KA and Eng C. The ERK1/2 pathway modulates nuclear PTEN-mediated cell cycle arrest by cyclin D1 transcriptional regulation. Hum Mol Genet 2006; 15: 2553-2559.
[6] Shen WH, Balajee AS, Wang J, Wu H, Eng C, Pandolfi PP and Yin Y. Essential role for nuclear PTEN in maintaining chromosomal integrity. Cell 2007; 128: 157-170.
[7] Zhao J, Chi J, Gao M, Zhi J, Li Y and Zheng X. Loss of PTEN expression is associated with high microRNA 24 level and poor prognosis in patients with tongue squamous cell carcinoma. J Oral Maxillofac Surg 2017; 75: 1449.e1-1449.e8.
[8] Ibrahim MY, Nunez MI, Harun N, Lee JJ, El-Naggar AK, Ferrarotto R, Wistuba I, Myers J, Glisson BS and William WN Jr. PI3-kinase pathway biomarkers in oral cancer and tumor immune cells. Head Neck 2019; 41: 615-622.
[9] Stambolic V, MacPherson D, Sas D, Lin Y, Snow B, Jang Y, Benchimol S and Mak TW. Regulation of PTEN transcription by p53. Mol Cell 2001; 8: 317-325.
[10] Hettinger K, Vikhanskaya F, Poh MK, Lee MK, de Belle I, Zhang JT, Reddy SA and Sabapathy K. c-Jun promotes cellular survival by suppression of PTEN. Cell Death Differ 2007; 14: 218-229.
[11] Virolle T, Adamson ED, Baron V, Birle D, Mercola D, Mustelin T and de Belle I. The Egr-1 transcription factor directly activates PTEN during irradiation-induced signalling. Nat Cell Biol 2001; 3: 1124-1128.
[12] Gan YH and Zhang S. PTEN/AKT pathway involved in histone deacetylases inhibitor induced cell growth inhibition and apoptosis of oral squamous cell carcinoma cells. Oral Oncol 2009; 45: e150-154.
[13] Leonard MK, Kommagani R, Payal V, Mayo LD, Shamma HN and Kadakia MP. DeltaNp63alpha regulates keratinocyte proliferation by controlling PTEN expression and localization. Cell Death Differ 2011; 18: 1924-1933.
[14] Yang A, Kaghad M, Wang Y, Gillett E, Fleming MD, Dotsch V, Andrews NC, Caput D and McKeon F. p63, a p53 homolog at 3q27-29, encodes multiple products with transactivating, death-inducing, and dominant-negative activities. Mol Cell 1998; 2: 305-316.
[15] Mangiulli M, Valletti A, Caratozzolo MF, Tullo A, Sbisa E, Pesole G and D'Erchia AM. Identification and functional characterization of two new transcriptional variants of the human p63 gene. Nucleic Acids Res 2009; 37: 6092-6104.
[16] Di Como CJ, Urist MJ, Babayan I, Drobnjak M, Hedvat CV, Teruya-Feldstein J, Pohar K, Hoos A and Cordon-Cardo C. p63 expression profiles in human normal and tumor tissues. Clin Cancer Res 2002; 8: 494-501.
[17] Sethi I, Romano RA, Gluck C, Smalley K, Vojtesek B, Buck MJ and Sinha S. A global analysis of the complex landscape of isoforms and regulatory networks of p63 in human cells and tissues. BMC Genomics 2015; 16: 584.
[18] Guo X, Keyes WM, Papazoglu C, Zuber J, Li W, Lowe SW, Vogel H and Mills AA. TAp63 induces senescence and suppresses tumorigenesis in vivo. Nat Cell Biol 2009; 11: 1451-1457.
[19] Celardo I, Grespi F, Antonov A, Bernassola F, Garabadgiu AV, Melino G and Amelio I. Caspase-1 is a novel target of p63 in tumor suppression. Cell Death Dis 2013; 4: e645.
[20] Bergholz J, Zhang Y, Wu J, Meng L, Walsh EM, Rai A, Sherman MY and Xiao ZX. DeltaNp63alpha regulates Erk signaling via MKP3 to inhibit cancer metastasis. Oncogene 2014; 33: 212-224.
[21] Wu G, Osada M, Guo Z, Fomenkov A, Begum S, Zhao M, Upadhyay S, Xing M, Wu F, Moon C, Westra WH, Koch WM, Mantovani R, Califano JA, Ratovitski E, Sidransky D and Trink B. DeltaNp63alpha up-regulates the Hsp70 gene in human cancer. Cancer Res 2005; 65: 758-766.
[22] Chae YS, Kim H, Kim D, Lee H and Lee HO. Cell density-dependent acetylation of DeltaNp63alpha is associated with p53-dependent cell cycle arrest. FEBS Lett 2012; 586: 1128-1134.
[23] Sasaki Y, Morimoto I, Ishida S, Yamashita T, Imai K and Tokino T. Adenovirus-mediated transfer of the p53 family genes, p73 and p51/p63 induces cell cycle arrest and apoptosis in colorectal cancer cell lines: potential application to gene therapy of colorectal cancer. Gene Ther 2001; 8: 1401-1408.
[24] Sayan BS, Yang AL, Conforti F, Bernardini S, Tucci P, Vasa-Nicotera M, Knight RA and Melino G. Induction of TAp63 by histone deacetylase inhibitors. Biochem Biophys Res Commun 2010; 391: 1748-1751.

[25] Gan Y, Shen YH, Wang J, Wang X, Utama B, Wang J and Wang XL. Role of histone deacetylation in cell-specific expression of endothelial nitric-oxide synthase. J Biol Chem 2005; 280: 16467-16475.
[26] Kou XX, Hao T, Meng Z, Zhou YH and Gan YH. Acetylated Sp1 inhibits PTEN expression through binding to PTEN core promoter and recruitment of HDAC1 and promotes cancer cell migration and invasion. Carcinogenesis 2013; 34: 58-67.
[27] Hao JQ, Li Q, Xu SP, Shen YX and Sun GY. Effect of lumiracoxib on proliferation and apoptosis of human nonsmall cell lung cancer cells in vitro. Chin Med J (Engl) 2008; 121: 602-607.
[28] Sheng X, Koul D, Liu JL, Liu TJ and Yung WK. Promoter analysis of tumor suppressor gene PTEN: identification of minimum promoter region. Biochem Biophys Res Commun 2002; 292: 422-426.
[29] Chen JH, Zhang P, Chen WD, Li DD, Wu XQ, Deng R, Jiao L, Li X, Ji J, Feng GK, Zeng YX, Jiang JW and Zhu XF. ATM-mediated PTEN phosphorylation promotes PTEN nuclear translocation and autophagy in response to DNA-damaging agents in cancer cells. Autophagy 2015; 11: 239-252.
[30] Bassi C, Ho J, Srikumar T, Dowling RJ, Gorrini C, Miller SJ, Mak TW, Neel BG, Raught B and Stambolic V. Nuclear PTEN controls DNA repair and sensitivity to genotoxic stress. Science 2013; 341: 395-399.
[31] Radu A, Neubauer V, Akagi T, Hanafusa H and Georgescu MM. PTEN induces cell cycle arrest by decreasing the level and nuclear localization of cyclin D1. Mol Cell Biol 2003; 23: 6139-6149.
[32] Danilov AV, Neupane D, Nagaraja AS, Feofanova EV, Humphries LA, DiRenzo J and Korc M. DeltaNp63alpha-mediated induction of epidermal growth factor receptor promotes pancreatic cancer cell growth and chemoresistance. PLoS One 2011; 6: e26815.
[33] Trotman LC, Wang X, Alimonti A, Chen Z, Teruya-Feldstein J, Yang H, Pavletich NP, Carver BS, Cordon-Cardo C, Erdjument-Bromage H, Tempst P, Chi SG, Kim HJ, Misteli T, Jiang X and Pandolfi PP. Ubiquitination regulates PTEN nuclear import and tumor suppression. Cell 2007; 128: 141-156.
[34] Xu L, Xing Q, Huang T, Zhou J, Liu T, Cui Y, Cheng T, Wang Y, Zhou X, Yang B, Yang GL, Zhang J, Zang X, Ma S and Guan F. HDAC1 silence promotes neuroprotective effects of human umbilical cord-derived mesenchymal stem cells in a mouse model of traumatic brain injury via PI3K/AKT pathway. Front Cell Neurosci 2018; 12: 498.
[35] Vazquez F, Ramaswamy S, Nakamura N and Sellers WR. Phosphorylation of the PTEN tail regulates protein stability and function. Mol Cell Biol 2000; 20: 5010-5018.
[36] Meng Z, Jia LF and Gan YH. PTEN activation through K163 acetylation by inhibiting HDAC6 contributes to tumour inhibition. Oncogene 2016; 35: 2333-2344.
[37] Kelpsch DJ and Tootle TL. Nuclear actin: from discovery to function. Anat Rec (Hoboken) 2018; 301: 1999-2013.
[38] McDonald D, Carrero G, Andrin C, de Vries G and Hendzel MJ. Nucleoplasmic beta-actin exists in a dynamic equilibrium between low-mobility polymeric species and rapidly diffusing populations. J Cell Biol 2006; 172: 541-552.
[39] Tang W, You W, Shi F, Qi T, Wang L, Djouder Z, Liu W and Zeng X. RNA helicase A acts as a bridging factor linking nuclear beta-actin with RNA polymerase II. Biochem J 2009; 420: 421-428.

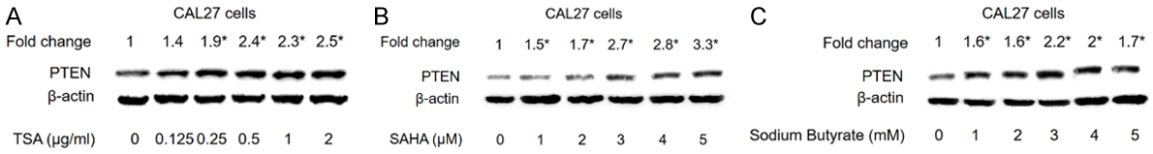

Figure S1. CAL27 cells were treated by TSA (A) or SAHA (B) or sodium butyrate (C) for 24 h and protein expression level of PTEN in was detected by western blot. *P < 0.05 versus the control groups.

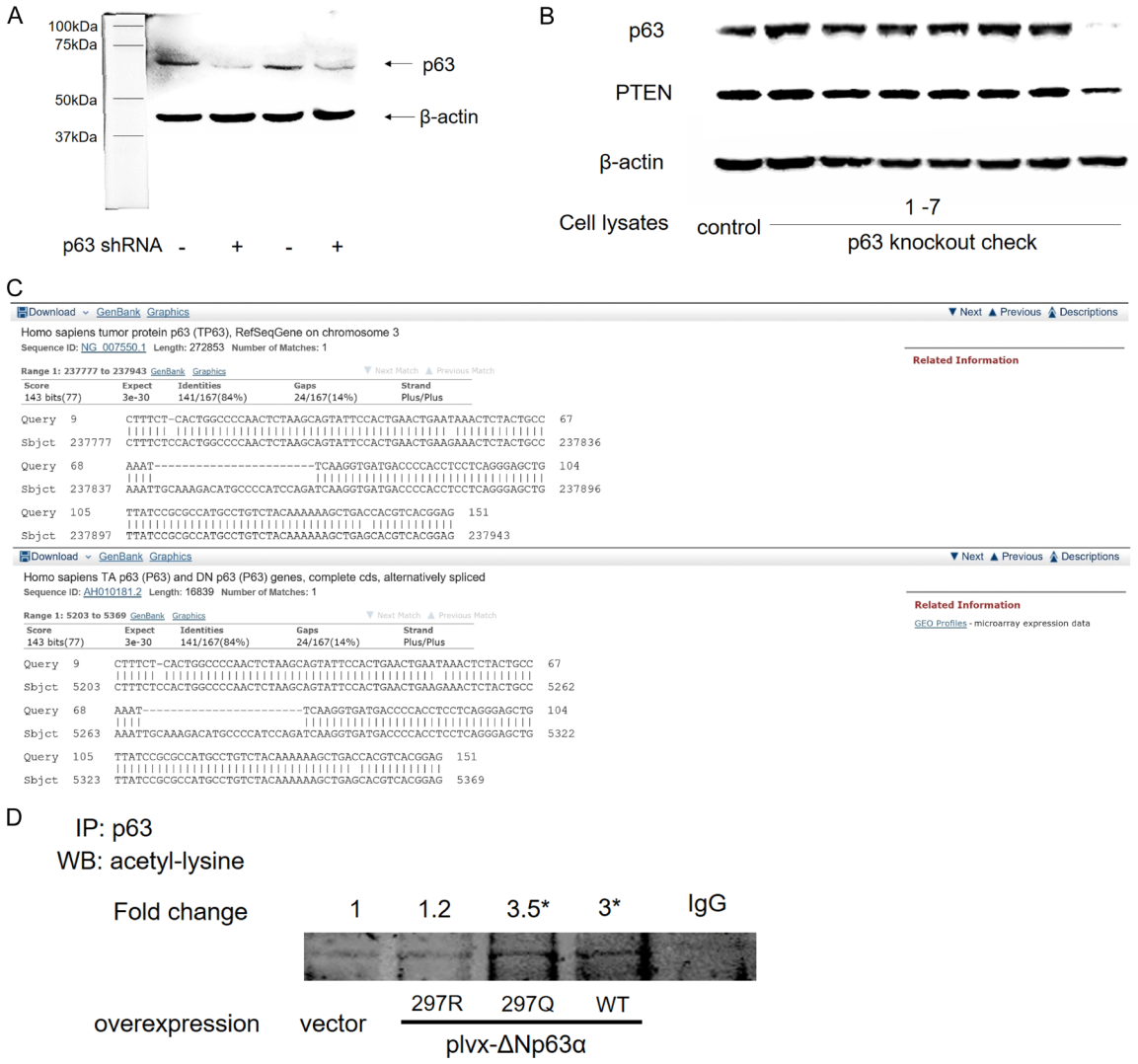

Figure S2. A. p63 were stably knockdown by lentivirus-mediated shRNA in WSU-HN6 cells. Two batches were showed. B. p63 were knockout in HeLa cells by CRISPR/Cas 9 and screened by western blot. C. BLAST of the PCR products targeting to p63 cut region by CRISPR/Cas 9. D. Wild-type ΔNp63α or K297 mutants were overexpressed in WSU-HN6 cells. Total protein was extracted and subjected to immunoprecipitation with an anti-p63 antibody and detected with an anti-acetyl-lysine antibody. Densitometry was performed to quantify scanned bands. Data was performed as fold changes compared with the control group. *P < 0.05 versus the control groups. IP, immunoprecipitation. WB, western blot.

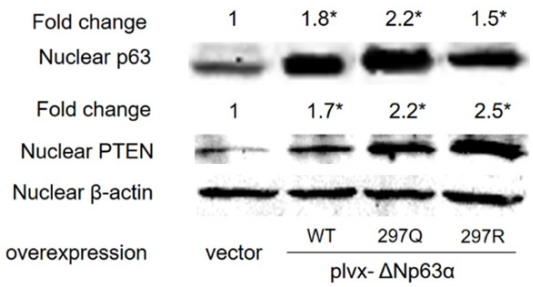

Figure S3. Wild type or K297 mutants were stably expressed in WSU-HN6 cells. Nuclear protein was extracted and subjected to western blot. B-actin was served as internal control for equal loading. Densitometry was performed to quantify scanned bands. Data was performed as fold changes compared with the control group. $^{*}P < 0.05$ versus the control groups.

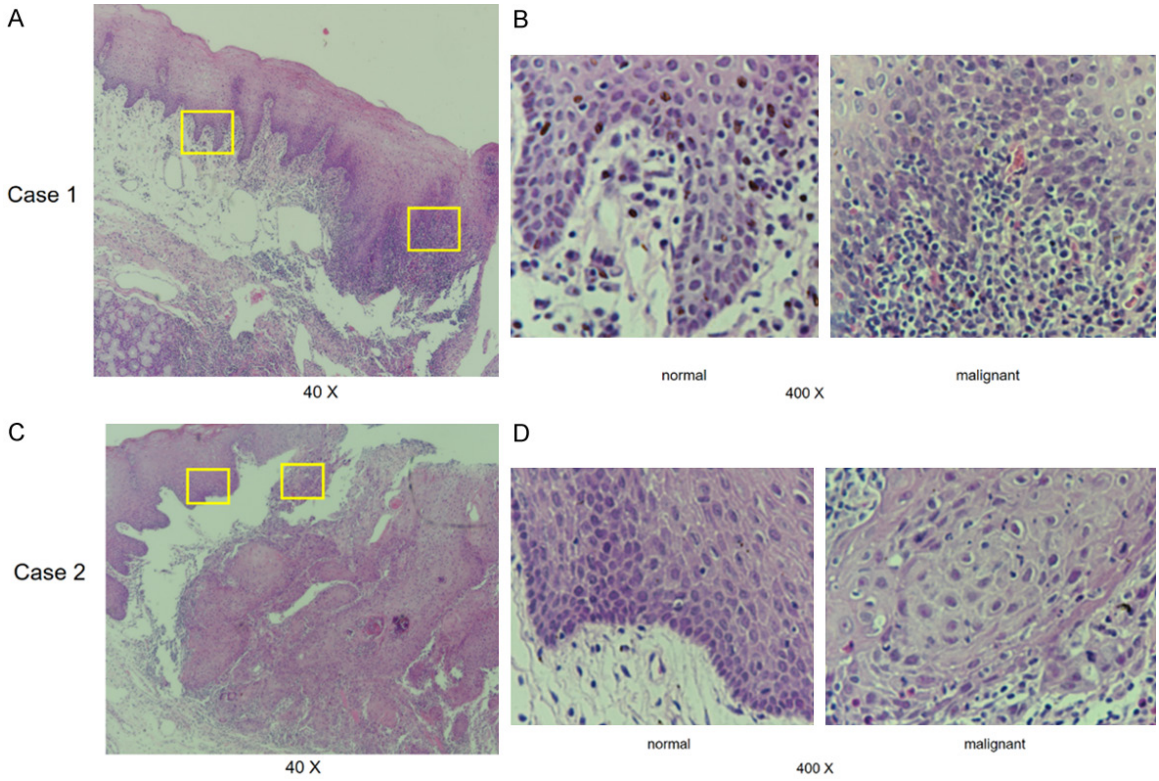

Figure S4. HE staining of normal and malignant area in pathological sections from tongue squamous cell carcinoma patients in **Figure 5**. (A) The same case with **Figure 5C**. (B) Magnified images of the rectangle frames of (A). (C) The same case with **Figure 5D**. (D) Magnified images of the rectangle frames of (C).

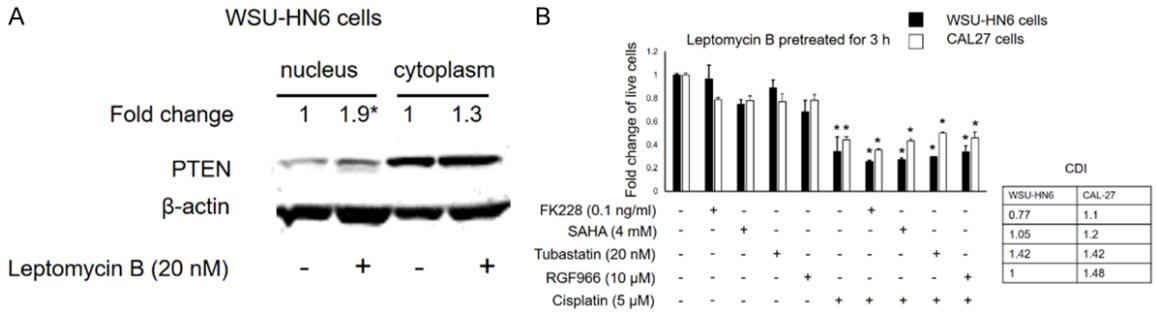

Figure S5. A. Nuclear PTEN was induced after treatment of leptomycin B for 48 h. Nuclear and cytoplasmic protein was separated and subjected to western blot. β-actin was served as internal control for equal loading. Densitometry was performed to quantify scanned bands. Data was performed as fold changes compared with the control group. B. WSU-HN6 cells or CAL27 cells were plated into a 96-well plate at 5000 cells/well and added leptomycin B for 3 h before treated with HDAC inhibitors listed respectively or cisplatin or cisplatin combined with HDAC inhibitors for 48 h. CCK-8 was performed to detect the amount of cells for each well. Data (mean ± SD of 5 separated experiments) were presented as relative living cells compared with the control groups. CDI, coefficient of drug interaction. $^{*}P < 0.05$ versus the control groups of the same series.

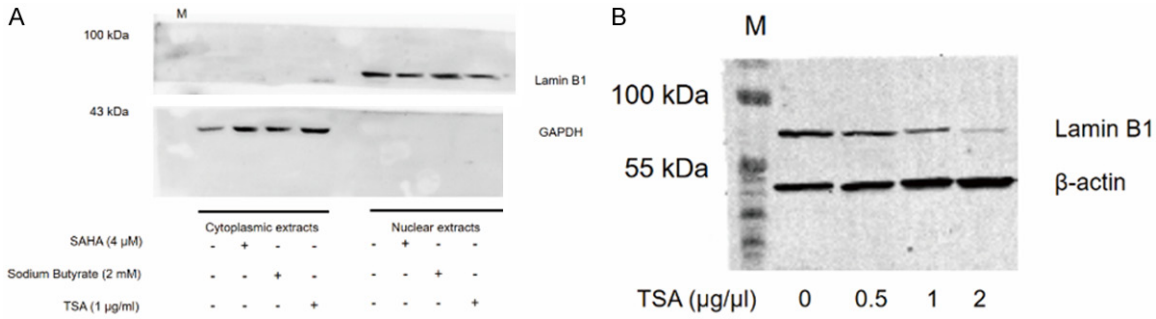

Figure S6. A. GAPDH and lamin B1 were examined to verify whether cytoplasmic contamination existed in nuclear extracts. Samples were the same as **Figure 7A**. Cells were treated with different HDAC inhibitors for 24 h, and subcellular components were separated and subjected to western blot analysis. Original images were showed and lttle cytoplasmic contamination was found in nuclear extracts. B. Lamin B1 was inhibited by a pan-HDAC inhibitor, TSA. Cells were treated with different dose of TSA for 24 h, and nuclear proteins were extracted and subjected to western blot analysis. Nuclear β-actin served as loading control. M, marker.